

Ubiquitylation is Required for Degradation of Transmembrane Surface Proteins in Trypanosomes

Wei-Lian Chung^{1,†}, Ka Fai Leung^{1,†},
Mark Carrington² and Mark C. Field^{1,*}

¹The Molteno Building, Department of Pathology,
University of Cambridge, Tennis Court Road, Cambridge
CB2 1QP, UK

²Department of Biochemistry, University of Cambridge,
Tennis Court Road, Cambridge CB2 1GA, UK

*Corresponding author: Mark C. Field, mcf34@cam.ac.uk

†These authors contributed equally to this work.

The surface of *Trypanosoma brucei* is dominated by glycosyl-phosphatidylinositol (GPI)-anchored proteins, and endocytosis is clathrin dependent. The vast majority of internalized GPI-anchored protein is efficiently recycled, while the processes by which transmembrane domain (TMD) proteins are internalized and sorted are unknown. We demonstrate that internalization of invariant surface glycoprotein (ISG)65, a trypanosome TMD protein, involves ubiquitylation and also requires clathrin. We find a hierarchical requirement for cytoplasmic lysine residues in internalization and turnover, and a single position-specific lysine is sufficient for degradation, surface removal and attachment of oligoubiquitin chains. Ubiquitylation is context dependent as provision of additional lysine residues by C-terminal fusion of neuronal precursor cell-expressed developmentally downregulated protein (NEDD)8 fails to support ubiquitylation. Attachment of NEDD8 leads to degradation by a second ubiquitin-independent pathway. Moreover, degradation of ubiquitylated or NEDDylated substrate takes place in an acidic compartment and is proteasome independent. Significantly, in non-opisthokont lineages, Rsp5p or c-Cbl, the E3 ubiquitin ligases acting on endocytic cargo, are absent but Uba1 class genes are present and are required for cell viability and ISG65 ubiquitylation. Hence, ubiquitylation is an evolutionarily conserved mechanism for internalization of surface proteins, but aspects of the machinery differ substantially between the major eukaryotic lineages.

Key words: endocytosis, intracellular transport, targeting, trypanosomes, ubiquitin, vesicle transport

Received 29 November 2007, revised and accepted for publication 19 June 2008, uncorrected manuscript published online 28 June 2008, published online 24 July 2008

Internalization of membrane proteins from the eukaryotic cell surface typically requires either recognition of a peptide-based sorting signal within the cytoplasmic domain or concentration within a membrane microdomain based on physicochemical and other properties. Lipid

microdomains are commonly associated with endocytosis of glycosyl-phosphatidylinositol (GPI)-anchored proteins, and at least two distinct modes have been described (1). Multiple cytoplasmic sorting signals have been identified for many surface proteins, most of which facilitate recognition by cytosolic adaptin protein (AP) complexes or other adaptors, and frequently conform to motifs containing tyrosine (NPXY/YXXØ) and/or dileucine ([DE]XXXL[LII]) sequences (2).

A more recently recognized internalization pathway is provided by modification by covalent attachment of ubiquitin. This process is mediated, in higher eukaryotes, by the action of an E3 ubiquitin ligase, typically Rsp5p or c-Cbl (3,4); the actions of the E3 ligases are themselves predicated on initial activation of ubiquitin by conjugation to an E1 protein and transfer of the ubiquitin molecule either by an E2 enzyme or directly by the E3 enzyme to the substrate polypeptide (5). The E3 enzymes act initially at the plasma membrane where ubiquitylation may occur in response to ligand engagement by a receptor (6,7). Recognition of the ubiquitylated molecules is mediated by several factors that contain a ubiquitin-interacting motif (UIM), for example epsin and eps15 (3). As epsin also binds to clathrin, this represents at least one mechanism by which ubiquitylated molecules may be internalized by conventional clathrin-dependent pathways (8). The affinity of individual UIMs for ubiquitin is in the low millimolar range and suggests a requirement for multiple interactions to facilitate stable association (9). Ubiquitylation of the adaptor molecules themselves may serve to produce such a network of interactions (10–13). In addition, modification by additional ubiquitin-like molecules, including the neuronal precursor cell-expressed developmentally downregulated protein (NEDD)8, can also promote internalization and degradation of surface molecules; much of the machinery for NEDDylation and ubiquitylation appears shared (14).

Ubiquitylated molecules are delivered to the lysosome for degradation by the multivesicular body (MVB). This process requires the activity of a group of proteins known as the endosomal sorting complex required for transport (ESCRTs). In *Saccharomyces cerevisiae*, all ESCRT factors are characterized as members of the class E vacuolar protein sorting group. Inactivation of ESCRTs in metazoan systems leads to an enlarged endosomal structure, likely corresponding to the MVB, and to stabilization of ubiquitylated receptors (reviewed in 15). ESCRT complexes carry out multiple functions, including recognition of ubiquitylated molecules, association with the endosomal membrane

through recognition of phosphatidylinositol 3-phosphate and membrane deformation to create the inner vesicles that characterize the MVB. Co-ordinated assembly and disassembly of ESCRT complexes are important for maturation of endosomes, and in particular for sorting, deubiquitylation and ultimate delivery of internalized cargo to the lysosome (16).

The core membrane trafficking elements are highly conserved across the eukaryotic lineages, but a number of lineage-specific features, modifications, expansions and secondary losses accompanied the radiation of the eukaryotes (17,18). Relevant to endocytosis is the restriction of caveolin to metazoan systems, especially interesting as many protist taxa have a heavy emphasis on GPI anchors as a mode for membrane attachment (19). *Trypanosoma brucei* is both a pathogenic protozoan and a highly divergent eukaryote. The intracellular trafficking system in this organism is well studied on account of roles in immune evasion (reviewed in 20) and cell surface dominance by the GPI-anchored variant surface glycoprotein (VSG). The basic architecture of the trypanosome endocytic system is similar to that of higher eukaryotes but with several distinct features. Commonalities include Rab5, Rab7 and Rab11 functions and dileucine signal-based lysosomal targeting, the presence of MVBs and the importance of clathrin in endocytic events (20–23). Unusual features are the 90% predominance of GPI-anchored molecules, absence of an AP-2 complex, lack of a clear role for dynamin in mammalian-stage endocytosis and exclusive reliance on clathrin-mediated uptake (22,24). While detergent-resistant membrane fractions containing VSG have been described (25), the absence of caveolin, AP-2 and an essentially saturating density of VSG at the surface indicates that the initial endocytic event is likely non-selective, that is that concentration of specific molecules into clathrin-coated pits is not detected (26). Sorting endosomes exclude VSG from regions of the membrane-bearing clathrin coats, suggesting that sorting of VSG from other endocytic cargo may occur at internal sites, but the molecular basis for this is not known (26).

The major transmembrane domain (TMD) proteins at the trypanosome surface are the invariant surface glycoproteins (ISGs) (27). While these molecules have no known function, they are present on both cell surface and endosomal membranes and turn over significantly more rapidly than VSG, suggesting differential sorting (28). In this study, we demonstrate a hierarchical role for cytosol-disposed lysine residues in the C-terminal domain and further, that these residues may be covalently modified by ubiquitin, with the construction of oligoubiquitin chains. There is a well-conserved E1 ubiquitin activation system present in trypanosomes, but surprisingly, homologues of the E3 ubiquitin ligases responsible for modification of endocytic proteins in higher eukaryotes are absent from the genome, indicating considerable mechanistic divergence between trypanosomes and higher eukaryotes. In the accompany-

ing paper, we show that this mechanistic distinctiveness extends to the ESCRT system.

Results

A hierarchical role for cytoplasmic domain lysine residues in localization in trypanosomes

We previously demonstrated that the cytoplasmic domain of ISG65 is both necessary and sufficient for plasma membrane and endosomal targeting on account of redirection of BiPN, an irrelevant normally secreted hemagglutinin (HA)-tagged fusion protein, to the trypanosome plasma membrane and endosomes (28). The localization of the BiPNTm fusion protein is highly similar to that of endogenous ISG65 and hence facilitates modeling of TMD protein trafficking (Figure 1B). Furthermore, lysine residues within the BiPNTm cytoplasmic tail are required for endosomal targeting.

The C-terminus of ISG65/BiPNTm contains three highly conserved lysines (Figure 1A); two of which are comparatively close to the C-terminus, while the third is more proximal to the hydrophobic membrane-spanning region. We created a set of point mutants where each lysine (K) was replaced in turn by arginine (R) and investigated the effect of these substitutions on location and protein stability. Replacing any one lysine had no detectable effect on the location of BiPNTm, which remained colocalized with the early endosome marker Rab5A and partly with the recycling endosomal marker Rab11 (28). Initially, we observed that replacing either both the N-terminal lysine residues (RRK) or the N- and C-terminal lysines (RKR) resulted in no detectable alteration to the location of BiPNTm, as determined by immunofluorescence of permeabilized cells (Figure 1C). In contrast, replacing both C-terminal lysine residues in the KRR mutant resulted in a clearly decreased internalization efficiency, with diffuse surface staining present and only residual endosomally located BiPNTm.

Substitution of those lysine residues that led to greater surface expression, as determined by immunofluorescence, correlated with a significantly increased stability for the BiPNTm mutant protein (Figure 2). Cells expressing various mutant isoforms of BiPNTm were treated with cycloheximide to inhibit ongoing protein synthesis, and residual levels of BiPNTm were determined by Western blotting with anti-HA antibodies (Figure 2). The wild-type protein (KKK) has a very short half-life of less than 1 h, while removal of all three lysine residues (RRR) stabilized the protein, resulting in a half-life increase of ~400%. Furthermore, both the RRK and the RKR isoforms have similar stability to the wild-type KKK, but the KRR mutant is similar to the RRR form, with a half-life in excess of 3 h. A minor difference in stability between RRR and KRR may indicate residual contributions from the N-terminal-most cytoplasmic lysine.

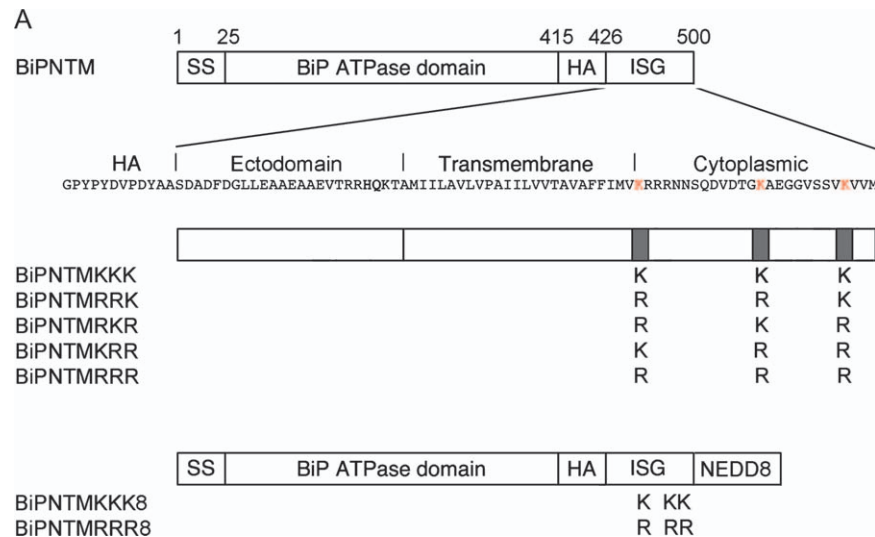


Figure 1: Role for cytoplasmic lysine residues in internalization of surface proteins in trypanosomes. A) Schematic of the TMD and cytoplasmic tail of ISG65/BiPNTm. BiPNTm consists of an N-terminal signal sequence (SS), BiP adenosine triphosphatase (ATPase) domain, an internal HA epitope, followed by C-terminal region of ISG65. The presence of the three conserved lysine residues within the cytoplasmic domain are indicated in red. Substitutions of residues in the BiPNTm lysine-to-arginine mutants are indicated. Similarly, conserved lysines and arginine substitutions in the BiPNTmNEDD8 constructs are also indicated. B) BiPNTm reporter (green) has an identical localization to ISG65 (red). Cell morphology was visualized using phase contrast, while DNA was visualized by co-staining with DAPI (blue). C) Location of BiPNTm fusion proteins. BiPNTm fusion proteins with two lysine-to-arginine point mutations were expressed in bloodstream-stage trypanosomes, and their location was determined in permeabilized cells and colocalized with Rab5A or Rab11, markers for early and recycling endosomes, respectively. RRR and RKR mutants are indistinguishable from the wild-type triple lysine construct (28), while the KRR isoform is mislocalized. Panels designated NP are non-permeabilized cells. Fusion protein was detected with mouse monoclonal anti-HA (green) and Rab5A or Rab11 with affinity-purified polyclonal antisera (red). Cells were counter stained for DNA with DAPI (blue). Scale bar is 2 μ m. Figure 1 continued on next page.

Internalization depends on the presence of the C-terminal lysine residues

To rigorously confirm a role for the cytoplasmic lysine residues in internalization, we subjected cells expressing mutant isoforms of BiPNTm to surface biotinylation using a membrane-impermeant biotinylation reagent. Surface (biotinylated) molecules were captured with streptavidin-conjugated beads, while non-biotinylated molecules were collected by trichloroacetic acid (TCA) precipitation. BiPNTm was quantified from both fractions by Western blot with anti-HA antibody. The wild-type construct, KKK, was predominantly recovered in the intracellular pool (soluble; S), with less than 20% disposed on the cell surface (biotinylated; B) (Figure 3). Both the single lysine forms RRR and RKR behaved identically to KKK, indicating that a single lysine at one of the two C-terminal positions is sufficient for efficient internalization. By contrast, removal of both C-terminal lysines (KRR) or all three (RRR) from the cytoplasmic tail resulted in a clear increase to the proportion of protein displayed at the surface. As a control, we also investigated the distribution of native ISG65 and found that approximately 50% was accessible to biotin, consistent with previous observations that the native protein is displayed more efficiently at the cell surface (28). To demonstrate that all the biotinylated material were cleared by the streptavidin beads, after binding to a first aliquot of

streptavidin beads, the resulting supernatant was incubated with a second aliquot of streptavidin beads. Our results show that all biotinylated material were recovered by the first aliquot of streptavidin beads (Figure S1).

Therefore, there is a clear correlation between the presence of a lysine residue in the second or third position of the cytoplasmic tail of BiPNTm, efficient uptake from the cell surface and a short half-life. In the absence of a lysine at one or other of these positions, BiPNTm is stabilized with increased presence on the cell surface. Taken together, this evidence suggests that lysine residues are required for both internalization and degradation of BiPNTm.

BiPNTm is covalently modified by ubiquitin

The clear importance of lysine residues in internalization and turnover of BiPNTm suggests that ubiquitylation is involved in the process. A role for ubiquitin-mediated turnover of trypanosome proteins in the control of the cell cycle has been suggested previously by studies on the role of the proteasome (29,30), but direct evidence for ubiquitylated proteins has not been reported.

The presence of ubiquitylated adducts of BiPNTm was detected directly by Western blot analysis with anti-ubiquitin

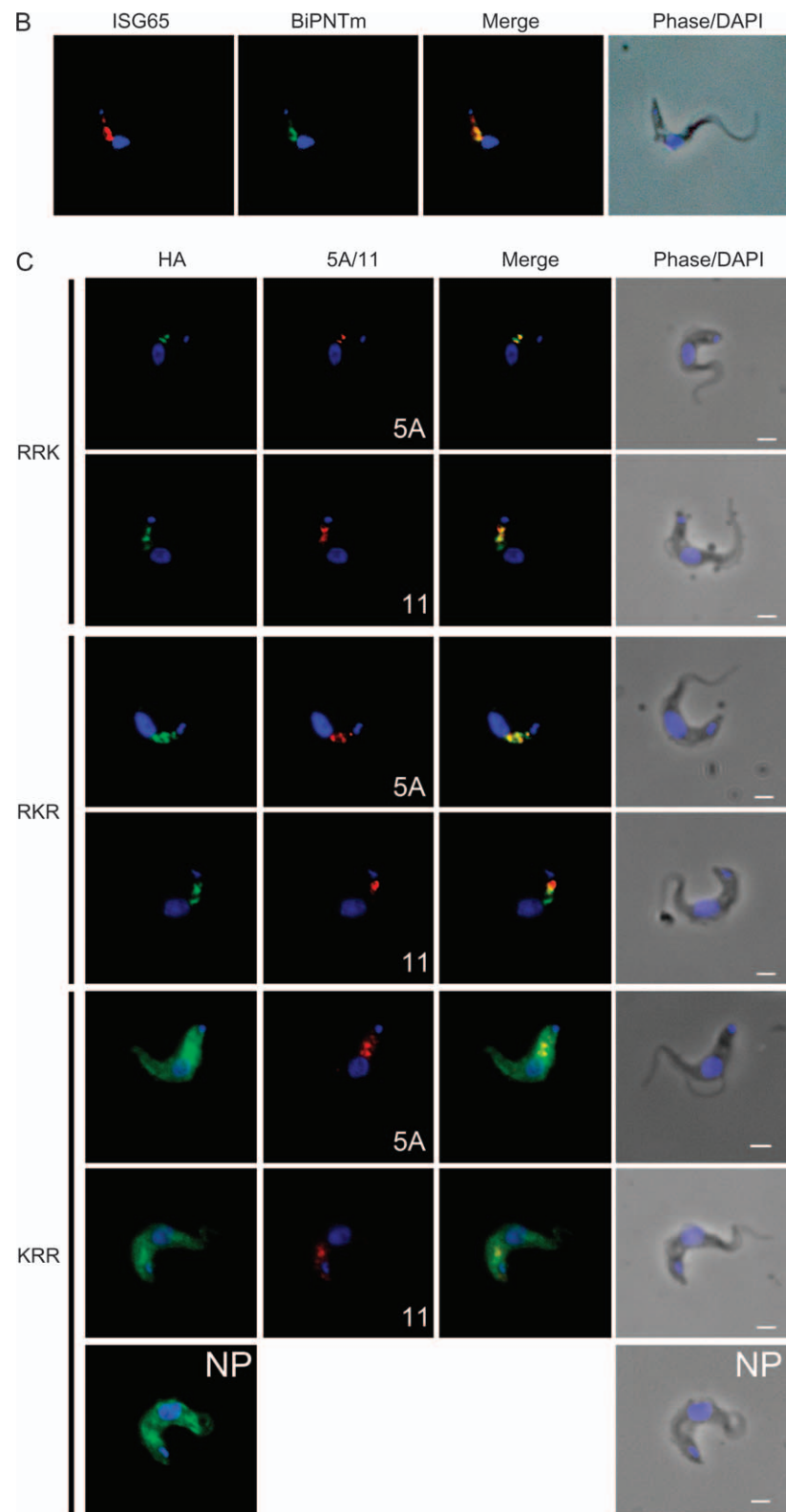


Figure 1: Continued from previous page.

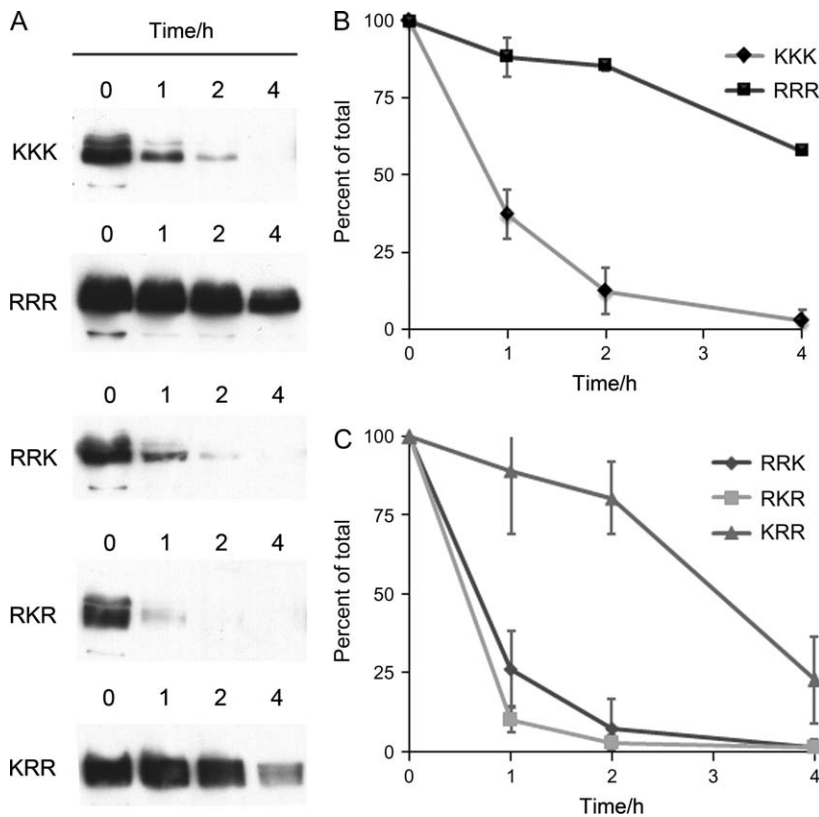


Figure 2: Turnover of BiPNTm is lysine dependent. A) Cells expressing various isoforms of BiPNTm were treated with cycloheximide to block ongoing protein synthesis, and the level of BiPNTm remaining was determined by Western blotting using anti-HA antibodies following solubilization and resolution by SDS-PAGE. Equivalence of loading was monitored for total protein in duplicate gels stained with Coomassie Blue or red Ponceau staining of the membrane prior to blocking. B and C) Quantification of replicate experiments as in (A) following densitometry. Each experiment was performed at least twice. Error bars indicate the standard error, and values are normalized to time zero.

antibody following immunoprecipitation of the fusion protein using anti-HA antibody (Figure 4A, lanes U; ubiquitin antibody blot). In lysates from cells expressing the wild-type form of BiPNTm (KKK), it was possible to detect up to five additional higher-molecular-weight bands, which likely correspond to ubiquitylated forms of BiPNTm (indicated by black dots in Figure 4). Both the RRK and the RKR forms produced similar patterns, suggesting that ubiquitylation can take place efficiently on each of the lysine residues close to the C-terminus. By contrast, lysates from the KRR mutant failed to show additional bands corresponding to ubiquitylated BiPNTm, despite the fusion protein having been captured as demonstrated when the lysate was probed with anti-HA (Figure 4A, lanes H; HA antibody blot). As a specificity control, neither the fusion protein nor the ubiquitylated adducts were detected in lysates of untransfected trypanosomes (Figure 4A, lanes 427). The heavy bands in lanes U result from detection of the HA antibody used in the immunoprecipitation, while two cross-reacting bands are detected with anti-HA in the cell lysates (Figure 4A, lanes 427).

To confirm the presence of covalently linked ubiquitin, cells expressing BiPNTmKKK were super-transfected with a second plasmid that expressed monomeric trypanosome ubiquitin, tagged at the N-terminus with the FLAG epitope. Transformants were selected, lysates prepared and proteins collected with anti-HA antibodies. These lysates

were probed with either anti-FLAG (Figure 4B, left panel) or anti-ubiquitin (Figure 4B, right panel) antibodies, while as a specificity control, wild-type cells (lanes 427) were treated in the same manner. FLAG antibodies clearly detected a ubiquitylated BiPNTm product at ~62 kDa, likely a monoubiquitylated adduct, as well as two higher-molecular-weight forms that were less abundant. Again, intense bands between 47 and 55 kDa correspond to detection of the anti-HA antibody used in the initial pull down. As further confirmation, lysates from cells expressing BiPNTmKKK and FLAG-ubiquitin were again subjected to anti-HA pull down, but the lysates were probed with anti-ubiquitin antibodies. A clear ladder of products with molecular weight greater than 62 kDa and highly similar to the pattern observed in panel A was obtained (Figure 4B, left panel).

Overall, these data demonstrate the covalent attachment of ubiquitin to BiPNTm. Furthermore, addition apparently can take place on either of the two C-terminal-most lysine residues, and these positions appear redundant as a similar pattern of ubiquitylated conjugates was obtained when either of these two lysines or both together were present. Finally, as up to five ubiquitylated products may be detected, even when only a single lysine is available for modification, oligoubiquitylation of BiPNTm lysine residues must be occurring, with chains containing at least five ubiquitin monomers.

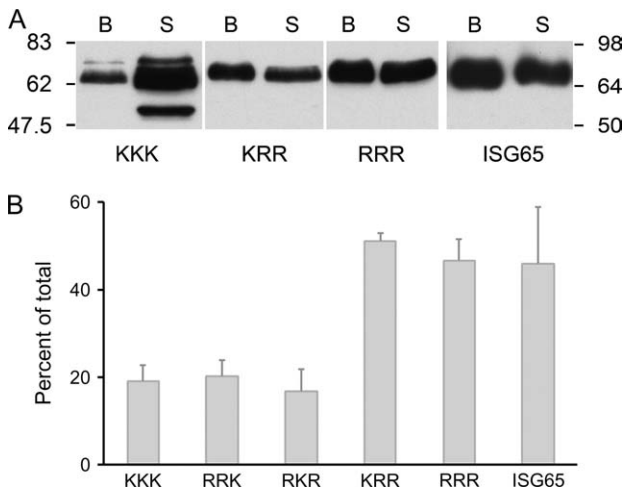


Figure 3: Surface location of BiPNTm is lysine dependent.

A) Western blot analysis of surface-biotinylated (lanes B) and non-biotinylated material (lanes S). Two-hundred-fold excess biotin (1 mM) was used to ensure that all surface molecules were biotinylated. Following biotinylation, the reactions were quenched, cells solubilized and biotinylated proteins captured with fivefold excess of streptavidin beads to ensure that all immune complexes were pulled down; non-biotinylated proteins were concentrated by TCA precipitation, and equivalent fractions were separated by SDS-PAGE and probed with anti-HA antibodies for BiPNTm or anti-ISG65. Migration positions of molecular weight markers are indicated at left for BiPNTm constructs and at right for ISG65. Equivalence of loading was monitored for total protein in duplicate gels stained with Coomassie Blue or red Ponceau staining of the membrane prior to blocking. B) Quantification of replicate experiments as in (A) following densitometry. Each experiment was performed at least twice. Error bars indicate the standard deviation.

Ubiquitylation is context dependent

To further probe mechanisms for degradation of BiPNTm, we attached the trypanosome ubiquitin-like protein NEDD8 to the C-terminus of BiPNTmKKK and -RRR isoforms to create BiPNTmKKK8 and BiPNTmRRR8, respectively. NEDD8 can be attached to mammalian cell surface proteins and lead to their downregulation by a mechanism that requires c-Cbl, the E3 ubiquitin ligase also responsible for ubiquitin conjugation (14). Significantly, NEDD8 and ubiquitin can be present on the same molecule, competing for the same lysine residues, but unlike ubiquitin, NEDD8 does not appear to form polymers. The NEDD8 BiPNTmKKK8 fusion protein retained the original C-terminal lysine residues of BiPNTm for potential conjugation as well as several additional lysine residues within its own sequence. The presence of covalently conjugated ubiquitin was monitored by pull down with anti-HA followed by Western blotting with anti-ubiquitin or anti-HA antibodies, while surface display was followed by biotinylation (Figure 5).

Wild-type cells (lanes 427) clearly contained no fusion protein or ubiquitylated forms, while in the cells expressing

BiPNTmKKK, we were able to detect multiple ubiquitylated forms. A pair of faint cross-reacting bands were detected by ubiquitin in the 427 lysates, which may be endogenous ubiquitylated proteins that were recognized by the anti-HA antibody. When the NEDD8 forms were analyzed, a new band at 62 kDa was observed, corresponding in molecular weight to BiPNTmNEDD8 (Figure 5A, left lanes). However, no new bands corresponding to ubiquitylated forms were detected, and moreover there was absence of a monoubiquitylated form, as detected for BiPNTmKKK (indicated on Figure 5A, second lane with a black dot), which would be expected to migrate just above the major BiPNTmNEDD8 band. Hence, BiPNTmNEDD8 fusion proteins are not major substrates for ubiquitylation.

Furthermore, the NEDD8 fusion proteins were very rapidly turned over with a half-life of less than 30 min (Figure 5B), and interestingly, this half-life was not influenced by the presence or absence of the lysine residues within the cytoplasmic tail of BiPNTm. This is fully consistent with the absence of both ubiquitylated conjugates and a role for ubiquitylation in turnover of these forms of BiPNTm. In addition, very little of either NEDD8 fusion protein isoform was found on the surface of trypanosomes, as assessed by biotinylation (Figure 5C), and the majority of detectable internal material colocalized with the early endosome marker Rab5A. Absence of colocalization with Rab11 suggests that these proteins are not, in the main, recycled. Overall, these data suggest that BiPNTmNEDD8 fusion proteins are highly unstable, efficiently internalized, do not recycle and are poorly expressed on the cell surface.

Degradation of TMD proteins is in an acidic compartment

To determine if the ultimate fate of TMD proteins included delivery to the lysosome for degradation, turnover of protein in cells expressing BiPNTm or the BiPNTmNEDD8 fusion protein was monitored (Figure 6). In higher eukaryotes, there is good evidence that ubiquitylated proteins are delivered to the terminal lysosome following passage through the MVB (15). However, at steady state, we were unable to detect lysosomally localized BiPNTm or ISG65 protein by co-staining with p67 (data not shown), potentially because of rapid degradation of any protein that reaches this compartment.

Treatment of cells with ammonium chloride clearly delayed turnover of BiPNTmKKK (Figure 6A,B, ammonium lanes), with a substantially less dramatic effect on the BiPNTmNEDD8 fusion protein, KKK8. Furthermore, the proteasome inhibitor MG132 did not protect either the BiPNTmKKK or the NEDD8 fusion protein. Taken together, these data suggest that ultimate disposal of the BiPNTm protein takes place in a low pH compartment, most probably the lysosome, and suggest no significant role for the proteasome in disposal of ubiquitylated protein within the trypanosome endosomal system.

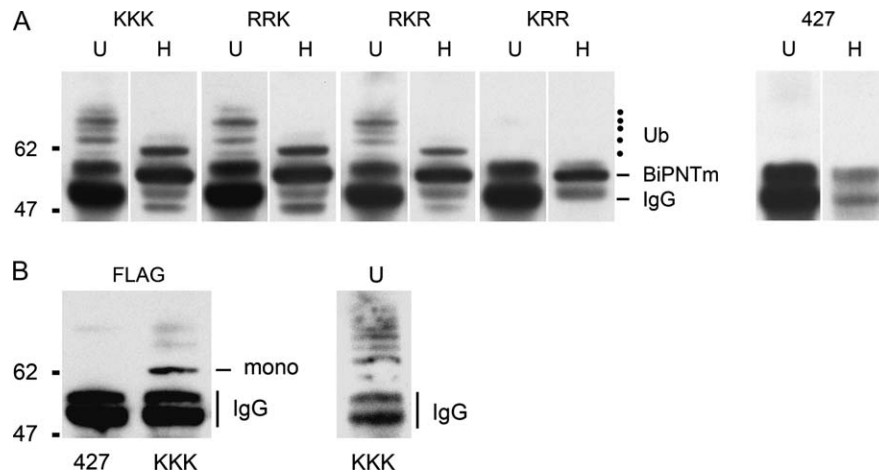


Figure 4: BiPNTm is modified by covalent attachment of ubiquitin. A) Lysates from BSF cells expressing HA-tagged BiPNTmKKK, -RRK, -RKR, -KRR or from control cells (lanes 427) were immunoprecipitated with anti-HA antibody, and the immunoprecipitates were separated by SDS-PAGE and then immunoblotted with anti-ubiquitin antibody P4D1 (denoted by U) and anti-HA antibody (denoted by H). The migration of unconjugated (BiPNTm) and conjugated (black circles) chimeric proteins are indicated on the right side as is the migration position of the IgG heavy chain, which is detected by the secondary antibody in the Western blot. B) Immunoblots of cells expressing FLAG-tagged trypanosome ubiquitin. Immunoprecipitated HA-tagged proteins from BiPNTmKKK (KKK) or from control cells (lane 427) also expressing FLAG-ubiquitin were probed with anti-FLAG antibody. Monoubiquitin-conjugated BiPNTm on the anti-FLAG blot is indicated as is the position of cross-reacting IgG heavy chain. Migration positions of molecular weight markers are indicated at left in kilodaltons.

Evolutionary divergence in the ubiquitylation machinery

To investigate further the role of ubiquitylation in endocytosis in trypanosomes, we searched for components of the ubiquitin transfer system. E3 ubiquitin ligases directly modify proteins with ubiquitin, and two are known to be involved in endocytosis. Rsp5p, a homologous to E6-AP carboxyl terminus (HECT) domain ubiquitin ligase, also containing a C2 domain and three WW domains, is involved in protein sorting and is associated with the MVB ESCRT complexes (31–33). Furthermore, Rsp5p localizes to multiple sites in the endocytic pathway, suggesting a role in ubiquitylation at various stages of endocytosis (34). The second well-characterized endocytic E3 ubiquitin ligase is c-Cbl, which ubiquitylates receptor tyrosine kinases, including the EGF receptor (35,36). c-Cbl contains an N-terminal tyrosine kinase-binding domain, a C₃HC₄ RING (really interesting new gene) finger domain, a proline-rich region and a C-terminal ubiquitin-associated (UBA) domain (37).

We searched the *T. brucei* genome with higher eukaryote Rsp5p or c-Cbl sequences. None of the HECT domain-containing candidates returned contained WW or C2 domains or BLASTed (reverse basic local alignment sequence tool) to Rsp5p in *S. cerevisiae* or to NEDD4 in *Homo sapiens*, the prototypical HECT family protein (38). Additional searches using Rsp5p without the HECT domain also failed to return a candidate with a predicted similar architecture or molecular weight to Rsp5p/NEDD4. Furthermore, phylogenetic analysis, using Bayesian inference, of all trypanosome HECT domain proteins indicated

no clear orthologous relationships to Rsp5p (data not shown). Similarly, several c-Cbl candidates were identified in the *T. brucei* genome, but none of these detected c-Cbl on reverse BLAST to the *H. sapiens* genome. We further examined all trypanosome open reading frames (ORFs) with predicted RING domains by phylogenetic reconstruction to identify those sequences closest to c-Cbl; none of these candidates had a similar domain architecture or successfully identified c-Cbl by reverse BLAST (data not shown). Altogether, this analysis suggests the absence of detectable orthologues of c-Cbl or Rsp5p in *T. brucei* and raises the possibility that alternate mechanisms or factors are utilized in divergent eukaryotes. Furthermore, we surveyed several additional genomes for the presence of Rsp5p and c-Cbl sequences [two Amoebozoa, four Archaeplastida, seven Chromalveolata and six Excavata, see accompanying paper (39)]; we were unable to detect such sequences in any genome outside the Opisthokonta, suggesting that these factors are highly restricted from an evolutionary standpoint (data not shown).

By contrast, E1 enzymes are highly conserved between trypanosomes and higher eukaryotes. In *S. cerevisiae*, there is a single E1, Uba1p (40), and the *H. sapiens* orthologue is UBE1 (41). We used Uba1p and UBE1 to search the trypanosome genome and identified two candidates, Tb927.8.2640 and Tb09.211.3610, with highly significant BLAST scores of 10^{-173} and 10^{-106} , respectively; (Figure S2) these ORFs are of similar size to Uba1 and reverse BLAST. The next most significant sequence was Tb927.5.3430, with an e value score of 10^{-29} . To confirm assignment of Tb927.8.2640 and Tb09.211.3610

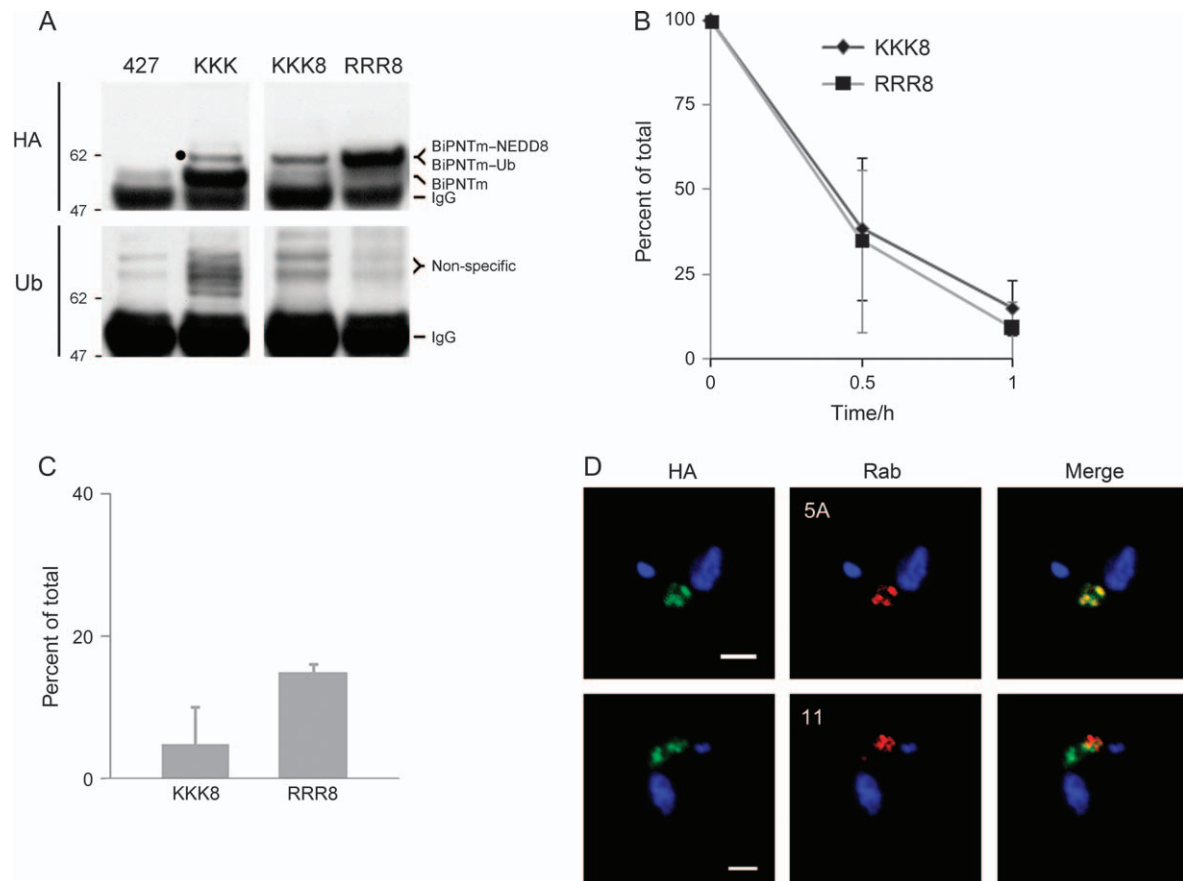


Figure 5: Ubiquitylation is context dependent. A) The trypanosome NEDD8 polypeptide (78 amino acid residues) was fused to the C-terminal end of BiPNTmKKK to create BiPNTmK88 or BiPNTmRRR to create BiPNTmRRR8. Lysates prepared from cells expressing these proteins were examined with anti-HA antibodies (upper panels). The BiPNTm migrates at ~55 kDa with a less intense band at 60 kDa (indicated with a black dot), likely the monoubiquitylated form. NEDD8 constructs KKK8 and RRR8 migrate with similar apparent molecular weight to monoubiquitylated BiPNTm (lanes KKK8 and RRR8). Anti-ubiquitin staining (lower panels) reveals ubiquitin conjugates in BiPNTmK88 but not in the NEDD8 forms (K88 and RRR8). A non-specific cross-reacting doublet is detected in the parental cell line (lane 427) negative control. B) Stability of NEDD8 constructs. Quantification of anti-HA reactivity in lysates of cells expressing the NEDD8 forms of BiPNTm with or without lysine residues following inhibition of protein synthesis with cycloheximide. The protein is considerably less stable than BiPNTm itself, but turnover is unaffected by the absence of potential ubiquitin acceptor sites in the cytoplasmic domain of BiPNTm. C) Surface biotinylation of cells expressing BiPNTmNEDD8 fusion proteins. Surface proteins were derivatized with membrane-impermeable biotin and quantified as described in *Materials and Methods* and Figure 3. The presence of the NEDD8 domain leads to significantly reduced surface expression. D) BiPNTmNEDD8 fusion protein is excluded from recycling endosomes. Cells expressing BiPNTmNEDD8 were immunostained with anti-HA (green), anti-Rab11 or Rab5A (red) and DAPI for DNA. Scale bar is 2 μ m. There is clear colocalization of the fusion protein with Rab5A but not with Rab11.

as Uba1-class orthologues, we performed a phylogenetic reconstruction using Tb927.8.2640, Tb09.211.3610, Tb927.5.3430 and members of the extended E1 family from *S. cerevisiae* and *H. sapiens* as reference sequences (Figure 7A). The data indicate that Tb927.8.2640 and Tb09.211.3610 encode Uba1-class proteins.

To demonstrate that the Tb927.8.2640 and Tb09.211.3610 ORFs are expressed, cells were transfected with tetracycline-inducible RNA interference (RNAi) constructs. RNAi of either Tb927.8.2640 or Tb09.211.3610 produced a significant growth defect after 2 days of induction compared with the non-induced cells (Figure 7B) (Table S1), while

messenger RNA (mRNA) expression and specificity of knockdown could be confirmed by quantitative real-time polymerase chain reaction (qRT-PCR) (Figure 7D). Furthermore, when cells harboring the RNAi construct for Tb09.211.3610 were induced with tetracycline and lysates probed with the ubiquitin-specific antibody FK2, there was a decrease of ~50% in the level of detectable ubiquitylated proteins (Figure 7C). Together, these data provide strong evidence that Tb927.8.2640 and Tb09.211.3610 encode functional Uba1-class factors required for cell cycle progression in trypanosomes and confirm the presence of highly conserved E1-related enzymes in these distant taxa. Furthermore, these data indicate that gene knockout

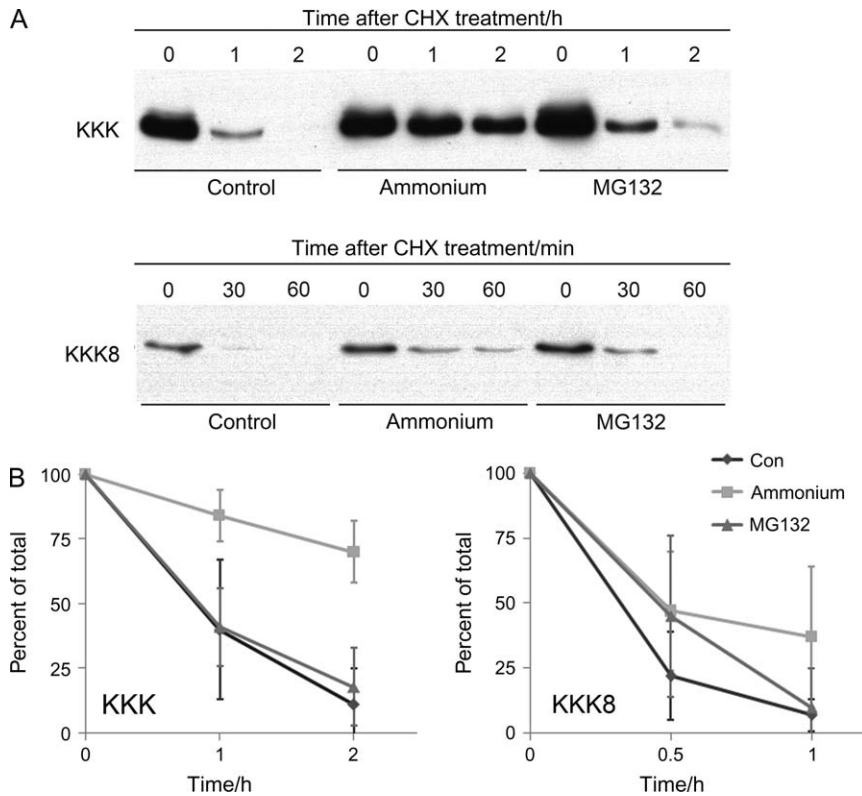


Figure 6: Degradation of ubiquitylated and NEDDylated proteins takes place in an acidic compartment.

A) Turnover of BiPNTm and BiPNTm-NEDD8 fusion proteins in the presence of a weak base (ammonium chloride) or proteasome inhibitor (MG132). Western blots of cells expressing BiPNTm or BiPNTmNEDD8 preincubated with the indicated inhibitor and then exposed to cycloheximide (CHX) to prevent ongoing protein synthesis. Fusion proteins were detected with anti-HA antibody. Equivalence of loading was monitored for total protein in duplicate gels stained with Coomassie Blue or red Ponceau staining of the membrane prior to blocking. B) Quantification of two experiments as in (A) by densitometry. Error bars represent the standard deviation, and values are normalized to time zero.

approaches are not possible for these ORFs as the growth defect by RNAi is consistent with essentiality. Therefore, we investigated the effect of knockdown of either Tb927.8.2640 or Tb09.211.3610 on turnover of endogenous ISG65. We were unable to observe any stabilization of the protein, despite obtaining significant suppression of the relevant mRNA (Figure 7D and data not shown), suggesting that there may be redundancy between Tb927.8.2640 and Tb09.211.3610 or that the level of knockdown was insufficient to elicit a clear phenotype. Consistent with this, it was recently shown in mammals that a second E1 enzyme, Uba6/UBE1L2, can also specifically activate ubiquitin, indicating a possible redundancy in ubiquitin activation by UBE1 family of proteins (42,43). However, it should also be noted that in mammalian cells, the level of protection of the EGF receptor in a ts40 background (Uba1 E1 knockout) is marginal despite efficient loss of function (14), and the predominant observation remains efficient turnover.

Double knockdown of both Uba1 E1 gene products leads to a severe growth phenotype

To demonstrate redundancy between the two E1 candidates, we generated a chimeric RNAi construct to specifically knockdown both E1 enzymes and transfected it into single marker bloodstream (SMB) cells. In the absence of RNAi induction, cells showed normal growth, with an approximate doubling time of 8 h as expected for wild-type cells (Figure S3, panel A). In contrast, cells subjected

to RNAi induction displayed a strong growth defect following 1 day of induction and remained so even after 7 days of induction. This growth defect was substantially more severe than that observed for knockdown of the individual E1 enzymes where a growth phenotype was only observed after the second day of induction (Figure 7B). Specific knockdown of Tb927.8.2640 and Tb09.211.3610 mRNA was demonstrated by qRT-PCR. Following 24 h of RNAi induction, Tb927.8.2640 mRNA was reduced by ~30% and Tb09.211.3610 mRNA by ~55% (Figure S3, panel B). Previous analysis of individual E1 mRNA levels was performed following 48 h of RNAi induction and displayed a stronger decrease in mRNA abundance (Figure 7D). We were unable to analyze cells induced beyond 24 h because of the severity of the RNAi phenotype. In addition to the growth defect, RNAi double knockdown resulted in severe morphological defects (Figure S3, panel C).

To determine whether RNAi double knockdown affected the steady-state levels of ISG65, cells were grown in the presence or absence of RNAi induction for 24 h, and cell lysates were probed by Western blotting with anti-ISG65 antibody. We were unable to observe a significant change in the levels of ISG65 in the presence of E1 double knockdown compared with control cells (Figure S3, panel D). However, we did observe a loss of ubiquitin-conjugated forms of BiPNTm in the presence of E1 double knockdown, strongly suggesting a role for the E1 enzymes in the ubiquitin pathway (Figure S3, panel E).

In conclusion, our data suggest that Tb927.8.2640 and Tb09.211.3610 are strong candidates for E1 enzymes and that they are likely to act in the same pathway.

Internalization of ISG65 is clathrin dependent

To determine if internalization of ISG65 requires clathrin, SMB cells harboring a clathrin RNAi construct were grown in the presence or absence of tetracycline and the localization and abundance of ISG65 were observed by immuno-

fluorescence and Western blotting. In non-permeabilized cells, ISG65 was found located on the surface of the plasma membrane in both non-induced and induced cells (Figure 8A). In permeabilized cells, ISG65 was found on vesicles likely to be of the early endocytic pathway, but there was a dramatic decrease in intracellular staining in cells subjected to clathrin RNAi. This was accompanied by the 'BigEye' phenotype as a result of enlargement of the flagellar pocket, as previously observed (22).

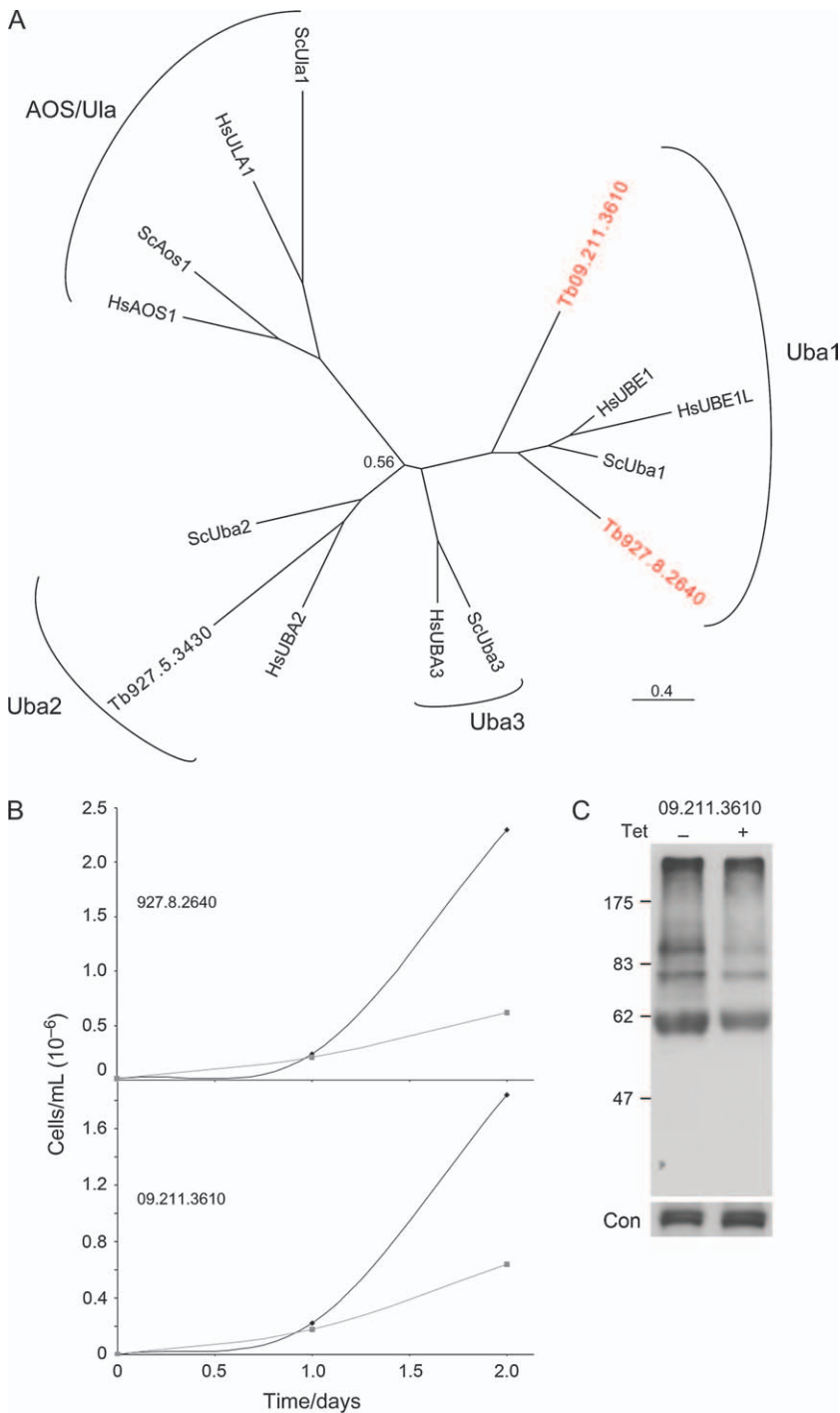


Figure 7: Trypanosome E1 ubiquitin ligases are required for cell cycle progression. A) Phylogenetic reconstruction using MRBAYES for Uba1-class ubiquitin-activating enzymes. The two most significant matches returned by BLAST searching of the trypanosome genome with E1 query sequences are included (red) together with reference sequences from *S. cerevisiae*, *H. sapiens* and the third hit from *T. brucei*. The phylogeny demonstrates that both Tb927.8.2640 and Tb09.211.3610 are Uba1 class. Statistical support (posterior probability) values are shown for nodes below 0.95. B) Knockdown growth analysis for trypanosome Uba1 ORFs. Cells were transfected with the relevant p2T7 RNAi construct harboring a 400- to 600-bp fragment specific to each ORF. Following selection (*Materials and Methods*), cultures were split and one aliquot was induced with tetracycline. Clear and significant growth defects were detected. C) Knockdown of Tb09.211.3610 results in decreased ubiquitin conjugation. Lysates from cells induced for Tb09.211.3610 RNAi were fractionated by SDS-PAGE, transferred to PVDF membranes and probed with monoclonal antibodies against ubiquitin (FK2). Filters were reprobbed with rabbit anti-clathrin heavy chain as a loading control. A decrease of ~50% in ubiquitin signal was detected following induction, indicating perturbation of the ubiquitylation pathway. D) Validation of E1 knockdown by qRT-PCR. mRNA was extracted from cells induced for RNAi of Tb927.8.2640 and Tb09.211.3610, and levels of mRNA were compared with non-induced controls and normalized against beta-tubulin. Error bars indicate standard error. Figure 7 continued on next page.

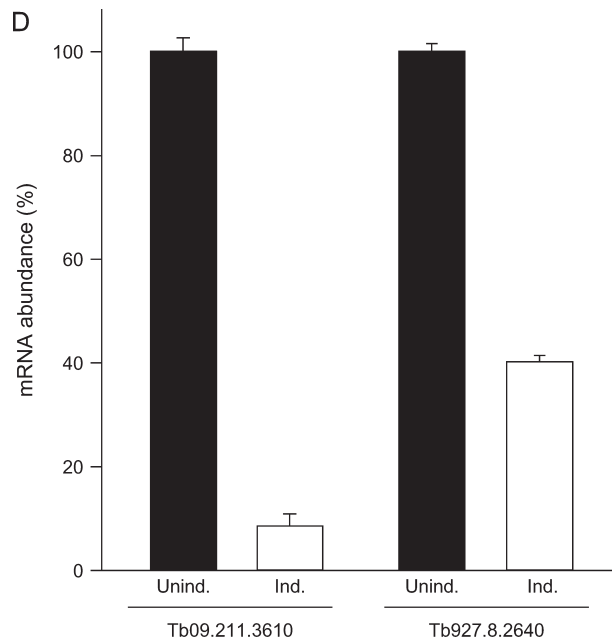


Figure 7: Continued from previous page.

Quantification of internal ISG65 staining indicated a significant decrease in the intracellular pool following clathrin RNAi (Figure 8B). To ensure that this reduced expression was not because of decreased global ISG65 expression, we determined ISG65 levels in whole lysates. These data indicate an ~40% increase in total ISG65 in clathrin RNAi cells, suggesting that ISG65 is stabilized and consistent with a block in endocytosis (Figure 8C). These data confirm that ISG65 internalization is clathrin dependent.

ISG65 does not contain extensive N-glycans

In trypanosomes, many glycoproteins present within the endosomal system have extensive processing of their *N*-glycans by addition of *N*-acetyl lactosamine repeats; significantly, there is evidence of a role for these structures in internalization of endocytic proteins, but these determinants appear to be absent from ISG65 based on affinity chromatography (44). We sought to investigate the state of the *N*-glycans on ISG65 to assess if these modifications could contribute to the internalization of the protein. Cells were cultured in the presence of tunicamycin, or lysates were treated with peptide *N*-glycanase (PNGase F) prior to analysis of the lysates by Western blot with anti-ISG65 antibodies (Figure 8D). Both these treatments resulted in increased mobility of the core protein by ~5 kDa, with a decrease in apparent molecular weight from ~65 to 60 kDa, indicating the likely presence of one or two ~2 kDa biantennary *M*-linked oligosaccharide chains and suggesting that ISG65 is not subject to extensive elaboration by lactosamine repeats, consistent with earlier work (44) and excluding an oligosaccharide-mediated pathway for ISG65 internalization.

Discussion

In trypanosomes, endocytosis has multiple features that differentiate the process from many organisms. These include utilization of a single clathrin-dependent, dynamin/AP-2-independent mechanism, unlike the multiple modes that operate in higher eukaryotes (22,24). Moreover, the surface is dominated by GPI-anchored proteins, at ~90% in terms of copy number, unusually placing TMD proteins as a small minority. However, endocytic traffic is differentiated, as evidenced by the presence of two distinct Rab5 early endosome populations (45) and two separate Rab4- and Rab11-dependent recycling pathways (46), while Rab21 and Rab28, two additional endosomal Rab proteins, are also present in trypanosomes (47) (J. Lumb and M. C. F., unpublished data). Taken together, this indicates considerable complexity, sorting and differential targeting.

Despite the number of pathways within the endosomal system, the primary endocytic event at the plasma membrane is non-concentrative as VSG density appears identical in clathrin-coated pits as a bulk surface membrane. Sorting likely occurs within intracellular compartments where VSG is efficiently excluded from clathrin-coated budding structures on endosomal structures (26); the mechanism for this process is not known. A sorting signal closely resembling the dileucine-based motif found in higher eukaryotes targets the trypanosome lysosomal protein p67, although the recognized sequence element appears rather more extensive than in metazoa (21,23). There is also evidence for carbohydrate-mediated endosomal targeting (44). Based on this and other evidence, it is assumed that GPI-anchored proteins are sorted by a default pathway, which accomplish an efficient endocytosis and recycling itinerary. This pathway also ensures minimal turnover for GPI-anchored proteins as VSG is degraded with a half-life in excess of 250 h (48). This huge excess of GPI-anchored proteins in trypanosomes and the absence of AP-2 from the genome raise the question of how TMD proteins are recognized and sorted by the trypanosome, especially as the most abundant cell surface TMD proteins ISG65 and ISG75 (27) lack obvious peptide motif-based endocytic targeting signals. However, the cytoplasmic domain of ISG65 is sufficient and necessary for endosomal targeting (28). The mechanism for ISG sorting must be highly efficient and discriminatory as turnover of VSG is some 40 times slower than that of ISG65 (the latter at 3–4 h) and ISG65 is sorted against a >100-fold VSG excess. This efficiency is even more remarkable as all endocytosis takes place from the flagellar pocket, representing <5% of the cell surface, and recycling is restricted to a comparatively small number of endosomes (20).

We find that the presence of lysine residues in the cytoplasmic domain of BiPNTm leads to both decreased surface expression and shorter half-life and that this phenomenon is position specific. Furthermore, we

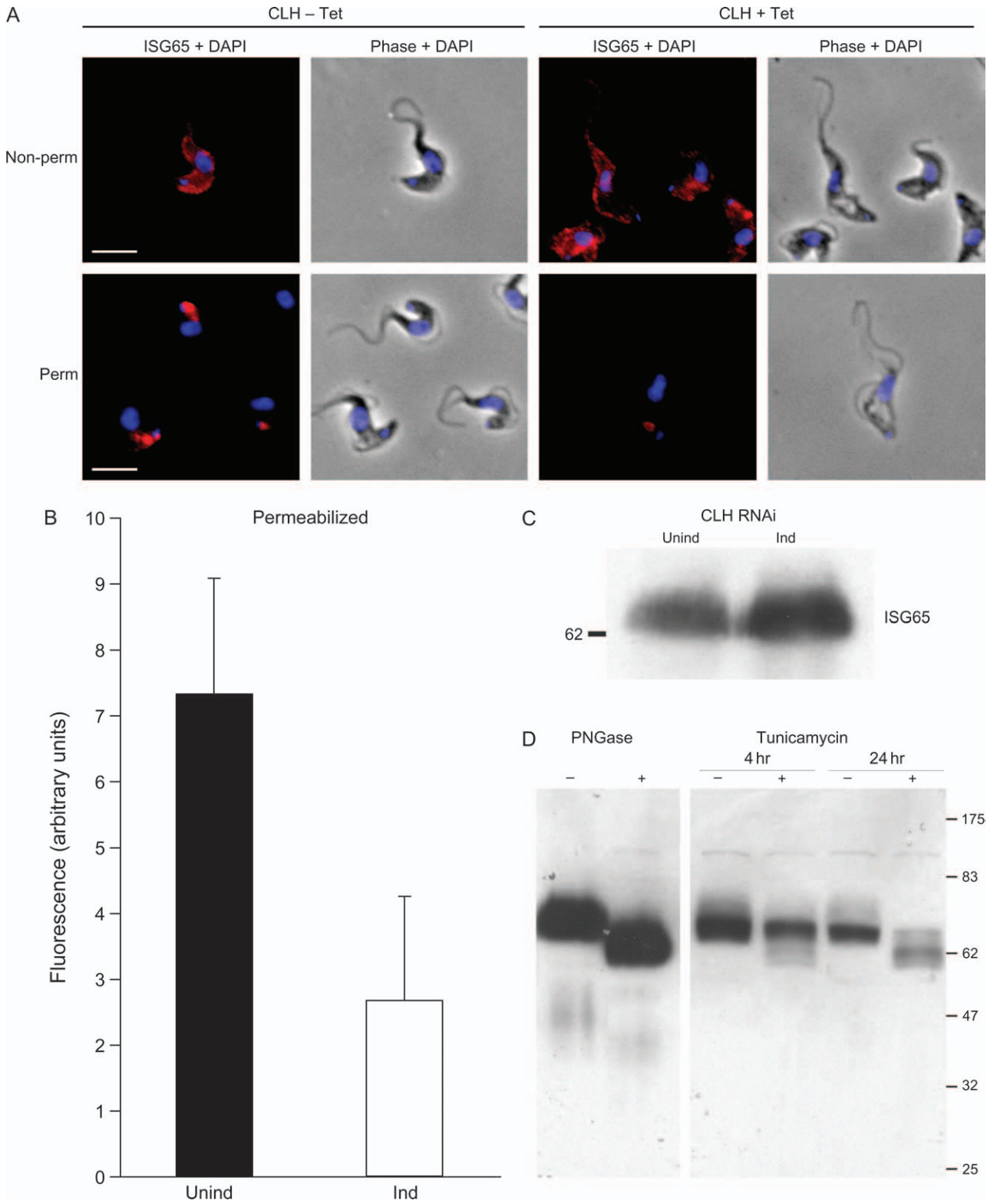


Figure 8: Legend on next page.

demonstrate covalently conjugated ubiquitin in BiPNTm adducts both by immunoprecipitation/Western blotting and by incorporation of a FLAG epitope-tagged ubiquitin into BiPNTm. Incorporation of ubiquitin requires the presence of either of the two lysine residues proximal to the C-terminus of the protein and is specific in that a third lysine residue in the cytoplasmic region, but closer to the membrane-spanning domain, appears to play a very minor role. Both C-terminal lysine residues support addition of at least five ubiquitin monomers. Several studies have demonstrated that monoubiquitylation is sufficient for internalization and degradation (35,49), but our findings are consistent with a recent study demonstrating that oligoubiquitylation provides an efficient internalization signal preferentially recognized over monoubiquitylated conjugates by UIM-containing endocytic adaptors (50). As this configuration is conserved between metazoa and trypanosomatids, it is potentially ancient and may represent the system present in the last common eukaryotic ancestor. Significantly, ubiquitylation patterns are very similar regardless of which C-terminal lysine residue is available, suggesting functional redundancy. Furthermore, we also show that internalization of ISG65 requires the presence of clathrin. This is not surprising because all endocytosis in bloodstream form (BSF) *T. brucei* that has been measured is clathrin dependent (22). However, our results appear to rule out an oligosaccharide-mediated pathway. This indicates that the ubiquitin-mediated pathway functions in concert with clathrin. Furthermore to this, the trypanosome orthologue of epsin appears to be important for the internalization of ISG65 (C. Gabernet-Castello and M. C. F., manuscript in preparation).

A high level of specificity for lysine recognition by the trypanosome ubiquitylation machinery is further supported by the demonstration that fusion of NEDD8 to the C-terminus of BiPNTm, which includes several lysine residues, fails to support ubiquitylation. While NEDD8 does not appear to support polymer formation in mammalian cells, its presence does not preclude ubiquitylation elsewhere on the host polypeptide and may even enhance it (14). Furthermore, NEDD8 and ubiquitin can use the same ligase, c-Cbl, for attachment in at least some cell types (14). Hence, these data suggest that the sequence environment surrounding the ubiquitin-accepting lysine residues in BiPNTm is important and shows that NEDDylation prevents ubiquitin conjugation at these sites. The obser-

vation that C-terminal fusion of NEDD8 severely destabilized BiPNTm, and that this turnover is not ubiquitin dependent, suggests that NEDD8 is capable of mediating a distinct surface protein downregulation pathway in trypanosomes. Interestingly, while this is rather similar to higher eukaryotes, the suppression of modification by ubiquitin of otherwise available lysine residues may suggest a distinctive aspect to this pathway in trypanosomes.

Overall, many of the features of ubiquitylation of surface molecules by trypanosomes destined for the endocytic system are shared with higher eukaryotes. Biochemically, turnover of ubiquitylated protein is insensitive to proteasome inhibition, but is inhibited by addition of mild base, strongly suggesting degradation in the lysosome. However, there are significant differences in terms of the factors that mediate these pathways. Specifically, ORFs encoding functional Uba1-class E1 ubiquitin-activating enzymes required for cell cycle progression can be confidently identified in the trypanosome, but homologues of the E3 ubiquitin transfer enzymes Rsp5 and c-Cbl mediating direct conjugation of ubiquitin to higher eukaryote endocytic proteins are absent from trypanosomes and other non-opisthokont genomes. This suggests that while the core of the system is conserved, some specific factors and elements are not retained. Hence, the cellular site and precise mechanism(s) of trypanosome ubiquitylation are likely distinct from higher eukaryotes. We previously noted the absence of conventional epsin and eps15 orthologues from the majority of eukaryote lineages, and most taxa possess the epsinR and eps15R forms, which lack a classical UIM (17). This further indicates evolutionary divergence within the ubiquitylation system, suggesting that trypanosomes, and probably many other lineages, mediate this pathway using distinct or divergent factors.

The evolutionary implications of conservation of general features of ubiquitylation but with apparent loss of multiple critical components are highly intriguing. In the accompanying paper, we demonstrate additional absences of important components of the ESCRT system (39), proteins responsible for targeting and sorting of ubiquitylated cargo through the MVB and on to the lysosome. Most pronounced is absence of the ESCRT 0 complex, involved in both recognition of ubiquitylated cargo and targeting of ESCRTs to the MVB, outside the Opisthokonta (16,51). Hence, absence of specific E3 ligases, UIM-containing

Figure 8: Internalization of ISG65 is clathrin dependent. A) Localization of ISG65 in the presence and absence of clathrin RNAi knockdown. SMB cells harboring the p2T7CLH construct were grown for 12 h in the presence or absence of tetracycline induction. The localization of ISG65 (red) was observed in non-permeabilized and permeabilized cells. DNA was visualized by co-staining with DAPI (blue). Scale bar = 2 μ m. B) Comparison of the fluorescence intensity of ISG65 staining in cells in the presence (open symbols) or absence (closed symbols) of clathrin knockdown. Clathrin RNAi results in a >50% decrease in the intracellular pool of ISG65 in permeabilized cells subjected to clathrin knockdown. C) Clathrin knockdown stabilizes ISG65. Cells subjected to clathrin RNAi were probed for ISG65. Densitometry indicates ~40% increase in total ISG65 in RNAi cells compared with control cells. D) Digestion of ISG65 with PNGase F or treatment with tunicamycin results in a small molecular weight shift. Cell lysates were digested with PNGase F overnight, while cells were exposed to tunicamycin for up to 24 h. ISG65 was detected in fractionated lysates using anti-ISG65 antibody.

epsin adaptors and the ESCRT 0 complex indicates that, despite conservation of a general use of ubiquitylation in endocytosis, there is considerable mechanistic diversity within ubiquitylation pathways across the different eukaryotic lineages.

Materials and Methods

Culturing of bloodstream forms of *T. brucei*

BSF trypanosomes were cultured in HMI-9 complete medium (HMI-9 supplemented with 10% heat-inactivated FBS, 100 U/mL penicillin, 100 U/mL streptomycin and 2 mM L-glutamine) (52) at 37°C with 5% CO₂ in a humid atmosphere in non-adherent culture flasks with vented caps. Cells were maintained at densities between 10⁵ and 5 × 10⁶ cells/mL. SMB line was used for the expression of tetracycline-inducible constructs (53). Ectopic expression of plasmid constructs was maintained with G418 and hygromycin B at 2.5 μg/mL, puromycin at 0.1 μg/mL and phleomycin at 1.0 μg/mL.

Plasmid constructs for overexpression and RNA interference

All constructs were verified by standard sequencing methods (Geneservice Ltd) prior to introduction into trypanosomes, and expression was further verified by Western blotting where appropriate. Primers for amplification of an RNAi target fragment were designed using the RNAi software tool (54). RNAi target fragments were PCR amplified using Taq DNA polymerase and genomic DNA template from 427 BSF cells with the following primers: for Tb927.8.2640, 26A RNAi-F (5'-CGCGCTTGACAATGTAGAAA-3') and 26A RNAi-R (5'-CCAAAAGAGGTCACCGTTGT-3'); for Tb09.211.3610, 211 RNAi-F (5'-GACCCTGACGTTGGAGTT-3') and 211 RNAi-R (5'-TGACACTTCTGAGCCAATGC-3'). E1 double knockdown construct (E1dKO) was generated by PCR amplification of two partially overlapping fragments: 26A RNAi-F and 26A dKO-R2 (5'-AACTCCACAACGTCAGGGTCAATCCCAAAGAGGTCACCGTTGT-3') primers were used for the first fragment, 211 dKO-F2 (5'-ACAACGGTGACCTCTTTGGGAATTCGACCGTTGTGGAGTT-3') and 211 RNAi-R for the second. Hundred nanograms of each fragment was then used as template for amplification of full-length E1dKO using 26A RNAi-F and 211 RNAi-R. PCR products were cloned into the tetracycline-inducible RNAi expression vector p2T7^{TAblue}, linearized with Eam11051. The p2T7LH clathrin heavy chain RNAi construct has been previously described (22). To generate double lysine/arginine (K-R) substitutions of BiPNTm, previously constructed single K-R mutants (28) were used as templates for PCR mutagenesis. From pXS5BiPNTmK2, primer pairs of RvK3 (5'-ACGGAATTCCTACTACTACTTTTACGCTAGAAACCCACCCCTCCG CACGTCCGGT-3') and FwBiPN (5'-ACGGAATTCACCCGGGAATTATG-3') or RvK4 (5'-ACGGAATTCCTACTACTACTCGCTACGCT-3') and FwBiPN were used to generate BiPNTm RRR (RRK) and BiPNTm RKR (RKR), respectively. The third isoform, BiPNTm KRR (KRR), was made from pXS5BiPNTmK3 with primers RvK4 and FwBiPN. All fragments were inserted into pXS5HA expression vector by using flanking *HindIII* and *EcoRI* restriction sites as described previously (28). To construct a FLAGTM-tagged ubiquitin, full-length TbUb was PCR amplified from *T. brucei* 427 strain genomic DNA. Primers FwFlagUb (5'-acgAAGCTTATGGACTACAAAGACGATGACG ACAAGATGCAGATCTTCGTGAAAACCTT-3'), which contains FLAG tag sequence, and RvFlagUb (5'-acgGAATTCcctACCACCTCGAAGACGAGCAC-3') were used to generate a 273-bp fragment of FLAG-tagged TbUb (FlagUb). The fragment was cloned into phleomycin-selective pXS5 expression vector yielding pXS5^{phleo}FlagUb. To create NEDD8-BiPNTm fusions, TbNEDD8 was amplified from genomic DNA by PCR with primers FwN8 (5'-ACGCCCGGCTTCTTAAGGTGAAGACTGTAAGC-3') and RvN8 (5'-ACGGAATTCAGCAACCCGCGCAGGG-3'), which contain restriction sites for *SmaI* and *EcoRI*, respectively. Fragments of the TMD of ISG65 (TmKKK) and its lysine-null mutant (TmRRR) were also amplified from previously constructed pXS5 plasmids with the following primers:

FwTM (5'-ACGGCTAGCGATGCTGACTTTGACTTTGACGGGTTG-3') and RvTMs (5'-ACGCCCGGCGATTACTACTTTTACGCT-3') for TmKKK and FwTM and RvTMRs (5'-ACGCCCGGCGATTACTACTCGCTACGCT-3') for TmRRR. Fragments of TmKKK or TmRRR, which were restricted by *SmaI* and *EcoRI* enzymes, together with TbNEDD8 were ligated into *NheI/EcoRI*-digested pXS5BiPN^{HA} vector.

Inhibitor treatment and glycosidase digestion

For analysis of glycosylation, trypanosomes were cultured in the presence of tunicamycin (Sigma) added to complete media at 1 μg/mL. For *N*-glycanase digestions, cells were lysed in 1% Nonidet P-40 (NP-40) in 100 mM sodium phosphate (pH 7.5) with complete protease inhibitor cocktail (Roche) heated to 95°C for 15 min and treated with 10 mU *N*-glycanase (New England Biolabs, NEB) overnight at 37°C; a second aliquot of *N*-glycanase was then added, and the reaction continued for 2 h prior to analysis by SDS-PAGE. For inhibition of the proteasome or lysosomal proteases, cells were cultured in the presence of 10 μM MG132 or ammonium chloride at 20 mM, respectively, for 1 h prior to initiation of the turnover analysis. Protein synthesis was inhibited by cycloheximide at 50 μg/mL.

Transfection

3 × 10⁷ cells (0.9–1.0 × 10⁶ cells/mL) per transfection were harvested at 800 × *g* for 10 min and washed with cytomix [2 mM EGTA (pH 7.6), 120 mM KCl, 0.15 mM CaCl₂, 10 mM K₂HPO₄/KH₂PO₄ (pH 7.6), 5 mM MgCl₂, 0.5% glucose, 100 μg/mL bovine serum albumin, 1 mM hypoxanthine and 25 mM HEPES (pH 7.6)]. Cells were resuspended in 400 μL of cytomix and transferred to a 2-mm gap electrocuvette containing 10–25 μg of linearized DNA plasmid. Electroporation was performed using a Bio-Rad Gene Pulser II (1.4 kV and 25 μF). Cells were transferred to a flask containing HMI-9 complete medium and allowed to recover at 37°C for 6 h. Antibiotic(s) was added for selection, and cells were subdivided into a 24-well plate. Positive clones were selected 5–6 days after transfection.

RNA interference and growth analysis

Following transfection with the relevant RNAi construct, clones were selected for hygromycin antibiotic resistance. RNAi was induced with 1 μg/mL tetracycline, which was added fresh daily. Cells were quantified using a Z2 Coulter Counter (Coulter Electronics) and maintained between 10⁵ and 5 × 10⁶ cells/mL.

Immunofluorescence analysis

Cells were harvested at 800 × *g* at 4°C for 10 min and washed with ice-cold Voorheis's-modified phosphate-buffered saline (vPBS; PBS supplemented with 10 mM glucose and 46 mM sucrose, pH 7.6) (55). Cells were then fixed in 3% paraformaldehyde in vPBS for 10 min at 4°C. Fixed cells were washed with ice-cold vPBS and applied to polylysine microscope slides (VWR International), sectioned with an ImmEdge Pen (Vector Laboratories, Inc.) for 20 min. For permeabilization, cells were incubated with 0.1% Triton-X-100 in PBS for 10 min at room temperature and washed three times for 5 min with PBS. Samples were blocked in 20% FBS in PBS for 1 h at room temperature. Fixed cells were incubated with primary antibodies for 1 h at room temperature, followed by three washes for 5 min in PBS. Secondary antibodies were then applied for 1 h at room temperature and washed as above. Samples were dried, and coverslips were mounted using Vectashield mounting medium supplemented with 4',6-diamidino-2-phenylindole (DAPI) (Vector Laboratories, Inc.). Coverslips were sealed with nail varnish (Max Factor Inc.). Antibodies were used at the following dilutions: mouse and rabbit anti-HA epitope immunoglobulin G (IgG) (both from Santa Cruz Biotechnology Inc.) at 1:1000, rabbit anti-ISG65 (from M. Carrington, Cambridge) at 1:1000, rabbit anti-Rab5A at 1:200, rabbit anti-Rab11 at 1:400 and mouse anti-p67 (from J. Bangs, Madison) at 1:1000. Secondary antibodies were used at the following dilutions: anti-mouse Oregon Green (Molecular Probes) at 1:1000 and anti-rabbit Cy3 (Sigma) at 1:1000. Specimens were examined on a Nikon Eclipse E600 epifluorescence microscope fitted with optically matched filter blocks and

a Hamamatsu ORCA charge-coupled device camera. Digital images were captured using METAMORPH software (Universal Imaging Corp.) on a Windows XP computer (Microsoft Inc.), and the raw images were processed using ADOBE PHOTOSHOP 7.0 (Adobe Systems Inc.). Fluorescence intensity was obtained by measuring the total intensity of a region of interest for 20 cells using the Region Measurements function on METAMORPH software and corrected by background subtraction.

Immunoprecipitation

Cells were pelleted at $16\,000 \times g$ for 15 seconds, washed in PBS and lysed by the addition of 100 μL of radioimmunoprecipitation assay (RIPA) buffer [25 mM Tris-HCl (pH 7.5), 150 mM NaCl, 1% NP-40, 0.5% sodium deoxycholate, 0.1% sodium dodecyl sulfate (SDS) and Complete Mini Protease Inhibitor Cocktail (Roche)] for 15 min on ice. Lysates were centrifuged for 30 seconds to remove nuclei and cell debris, and the supernatant transferred to a fresh tube. Thirteen microliters of 10% SDS was added to the supernatant and incubated at 95°C for 5 min. Samples were diluted with 750 μL of dilution buffer [50 mM Tris-HCl (pH 7.5), 1.25% Triton-X-100, 190 mM NaCl, 6 mM ethylenediaminetetraacetic acid (EDTA) and Complete Mini Protease Inhibitor Cocktail]. Thirty microliters of Pansorbin (Calbiochem) (prewashed and resuspended in dilution buffer) was added to the supernatant and incubated at 4°C for 1 h. Samples were centrifuged at $16\,000 \times g$ for 5 min and the supernatant transferred to a fresh tube. Two microliters of anti-HA antibody was added to each sample and incubated at 4°C overnight on a rotating device. Immune complexes were then isolated by the addition of 20 μL of protein A-Sepharose on a rotating device for 1 h at room temperature. Subsequently, Sepharose beads were washed twice with wash buffer I [50 mM Tris (pH 7.5), 0.1% Triton-X-100, 0.02% SDS, 150 mM NaCl and 5 mM EDTA] and twice with wash buffer II [50 mM Tris (pH 7.5), 0.02% Triton-X-100 and 1 M NaCl]. A further centrifugation step was performed for 15 seconds at $16\,000 \times g$, and the remaining supernatant was removed by pipetting. Samples were resuspended in $1 \times$ SDS sample buffer and denatured at 95°C for 5 min and subjected to 12.5% SDS-PAGE.

Protein electrophoresis and Western blotting

Trypanosomes were harvested and washed twice in PBS (Sigma). Pellets (1×10^7 cells) were lysed in 100 μL of boiling SDS sample buffer [10% (w/v) glycerol, 100 mM DTT, 3% (w/v) SDS, 0.01% (w/v) bromophenol blue and 50 mM Tris-HCl (pH 6.8)] and resolved by SDS-PAGE on 12.5% SDS-polyacrylamide mini gels. The proteins were electrophoretically transferred onto polyvinylidene fluoride (PVDF) membrane (Immobilon; Millipore) using a wet transfer tank (Hoefer Instruments). Non-specific binding was blocked with Tris-buffered saline with Tween-20 (TBST) [137 mM NaCl, 2.7 mM KCl, 25 mM Tris base (pH 7.4) and 0.2% Tween-20] supplemented with 5% freeze-dried milk. Commercial monoclonal anti-HA9 and P4D1 anti-ubiquitin antibodies (Santa Cruz Biotechnology) were used at 1:10 000 and 1:1000, respectively, and monoclonal anti-FLAG antibody was at 1:500. A rabbit polyclonal serum against anti-ISG65 antibody was diluted 1:10 000 in TBST milk. Incubations with commercial secondary anti-IgG rabbit or anti-IgG mouse horseradish peroxidase conjugates (Sigma) were performed at 10 000-fold dilution in TBST milk. Detection was by chemiluminescence with luminol (Sigma) on BioMaxMR film (Kodak).

Protein stability

Trypanosomes were cultured for up to 6 h in HMI-9 medium containing 50 $\mu\text{g}/\text{mL}$ cycloheximide (Sigma) to prevent translation. Samples were taken at different time-points and analyzed by Western blot. Data were quantified by scanning of X-ray films following chemiluminescence exposure, followed by analysis with IMAGEJ (<http://rsb.info.nih.gov/ij/>).

Biotinylation

10^7 mid-log phase cells were collected and washed three times in vPBS. Biotinylation was carried out in wash buffer supplemented with 200-fold excess (1 mM) EZ-link Sulfo-NHS-LC-Biotin (Pierce) for 1 h on ice. Surplus biotin was removed by three washes with ice-cold vPBS. Cells were

solubilized by incubating with lysis buffer [150 mM NaCl, 1% (v/v) Triton-X-100, 0.1% (w/v) SDS and 20 mM Tris-HCl (pH 7.4)] in the presence of protease inhibitors (Roche). After rolling at 4°C for 1 h, insoluble material was removed by centrifugation at $16\,000 \times g$ for 20 min at 4°C . Biotinylated proteins were separated from non-biotinylated proteins by adsorption to fivefold excess (50 μL) EZ-view™ Red Streptavidin Affinity Gel (Sigma; washed in lysis buffer). The cell extract and streptavidin gel slurry (10:1, v/v) were rotated for 4 h in the cold. After centrifugation at $16\,000 \times g$, the supernatant was saved and concentrated by TCA precipitation. The gel slurry was washed twice in wash buffer [130 mM NaCl, 5 mM KCl, 1 mM CaCl_2 , 1 mM MgSO_4 , 5 mM NaPO_4 and 20 mM HEPES (pH 7.1)], and bound proteins were eluted by boiling in SDS sample buffer, and both fractions were subjected to 12.5% SDS-PAGE and Western blotting. The blots were treated with either monoclonal anti-HA or rabbit anti-ISG65 antiserum and quantified using IMAGEJ software.

Bioinformatics

Trypanosomatid data were at the Sanger Institute Web site (<http://www.genedb.org/>) and were searched using BLAST. In addition, the predicted proteome for *T. brucei* was downloaded and searched using Smith-Waterman using CLC WORKBENCH v3.0.1 with Cube hardware acceleration (<http://www.clcbio.com/>) on a MacBook Pro (<http://www.apple.com/>). All recovered sequences were subjected to reverse BLAST/Smith-Waterman for confirmation of orthology. Alignments were done using CLUSTALX, and phylogenetic reconstruction was done using MRBAYES v3.1.2 (<http://mrbayes.csit.fsu.edu/>).

Cell cycle analysis

Estimates of cell cycle positions were done exactly as described (56).

Densitometry

All fluorographs were scanned at 16-bit gray scale resolution, and exposures were selected to ensure that the film was not saturated. In most cases, the exposures shown in the figures represent overexposed versions of the same data used in quantification. Quantification and background subtraction were then done with IMAGEJ (<http://rsb.info.nih.gov/ij/>).

Quantitative real-time polymerase chain reaction

1×10^8 cells were harvested at $3450 \times g$ for 10 min at 4°C and washed with ice-cold PBS. Cells were quick frozen in dry ice for 1 min, and RNA was purified using the RNeasy mini kit (Qiagen) according to the manufacturer's instructions. RNA concentration was quantified using a ND-1000 spectrophotometer and NANODROP software (Nanodrop Technologies). qRT-PCR was performed using iQ-SYBR Green Supermix on a MiniOpticon Real-Time PCR Detection System (Bio-Rad) and was quantified using OPTICON3 software (Bio-Rad). The following primers were used for qRT-PCR: for Tb927.8.2640, 26A RTF (5'-AACGCATTGCTGGAAGAATC-3') and 26A RTR (5'-CTGTGCAC-CATTCTCACGAT-3'); for Tb09.211.3610, 211 RTF (5'-GAATCGCACACATTTTACAG-3') and 211 RTR (5'-TTATTGTTGGATGCGCAAAA-3').

Acknowledgments

This study was supported by project and program grant funding from the Wellcome Trust. We thank Joel B. Dacks (Cambridge) for discussion of evolutionary aspects of this study, James Bangs (Madison) for antibodies, David Eastwood and Daniel Neil for contributions at the project's initiation.

Supporting Information

Additional Supporting Information may be found in the online version of this article:

Figure S1: Biotinylation efficiently recovers surface ISG65. Cells were subjected to surface biotinylation as described in *Materials and Methods* and

recovered with streptavidin beads. The supernatant was subjected to a second round of capture with a further aliquot of streptavidin-agarose. Lane T, total lysate; lanes B1 and B2, bead captures rounds one and two, respectively. Lysates were fractionated by SDS-PAGE and ISG65 detected with affinity-purified antibody. Numbers at left indicate the molecular weights and migration positions of coelectrophoresed standards in kilodaltons.

Figure S2: Alignment of E1 ubiquitin-activating enzymes from *H. sapiens*, *S. cerevisiae* and *T. brucei*. The alignment was done with CLUSTALX. '*' indicates identical amino acids, ':' indicates strongly conserved amino acids and '.' indicates weakly conserved amino acids. The underlined region is the ATP-binding motif, and the region in black is the active site containing the conserved cysteine for thiol ester formation with ubiquitin.

Figure S3: Characterization of E1 double knockdown bloodstream form cells in *T. brucei*. Trypanosomes were transfected with p2T7●E1d-KO, and transformants were isolated by antibiotic selection (*Materials and Methods*). A) Growth analysis for E1 double knockdown cells. Uninduced (closed symbols) and induced cells (open symbols) were grown over a period of 9 days, and cell numbers were monitored. A strong growth defect was observed following 1 day of RNAi induction. All subsequent experiments were conducted after 24 h of RNAi induction. Note that, by day eight, the RNAi system was broken and cells reverted to a normal mitosis phenotype. Similar data were obtained for multiple independent experiments. B) Validation of E1 knockdown by qRT-PCR. mRNA was extracted from cells, and levels of mRNA were compared with non-induced controls. mRNA abundance was detected using primers for either Tb927.8.2640 or Tb09.211.3610 and normalized against beta-tubulin. Error bars derive from duplicate experiments and show the standard deviation. C) Knockdown of both E1 enzymes results in severe morphological defects. Phase-contrast images of non-induced control cells and induced cells co-stained with DAPI (blue) to visualize DNA. Lower panels represent other examples of morphological phenotypes observed in induced cells. Scale bar is 2 μm . D) Steady-state levels of ISG65 were comparable between uninduced and induced cells. Three hundred nanograms of total protein lysate from non-induced and induced cells was subjected to SDS-PAGE, followed by Coomassie staining (lower panel) or Western immunoblotting with anti-ISG65 specific antibody (upper panel). Numbers indicate the molecular weight in kilodaltons. E) Double knockdown of E1 enzymes results in loss of ubiquitylated forms of BiPNTm. Lysates from BSF cells expressing HA-tagged BiPNTm in the presence or absence of E1 knockdown were immunoprecipitated with anti-HA antibody. Immunoprecipitates were separated by SDS-PAGE and then immunoblotted with anti-ubiquitin antibody P4D1 (denoted by U) and anti-HA (denoted by H). The migration of unconjugated (BiPNTm) and ubiquitin-conjugated (black circles) proteins is indicated on the right side as is the migration position of the IgG heavy chain, which is detected by the secondary antibody in the Western blot. Lower panel shows a longer exposure of immunoblots using anti-ubiquitin antibody. Numbers indicate the molecular weight in kilodaltons of co-electrophoresed marker proteins.

Table S1: RNAi knockdown of E1 ubiquitin ligase candidates results in a cell cycle block. Following induction, cells harboring RNAi plasmids were fixed, stained with DAPI and the copy number of the nucleus and kinetoplast determined. Data were obtained for >250 cells in each instance. For ORF 09.211.3610, a clear accumulation of cells that have completed mitosis but not cytokinesis is observed, consistent with a role in this event. Data are expressed as per cent (note: some analyses do not total 100% because of the presence of cells with organellar copy numbers not included here).

Please note: Wiley-Blackwell are not responsible for the content or functionality of any supporting materials supplied by the authors. Any queries (other than missing material) should be directed to the corresponding author for the article.

References

1. Mayor S, Riezman H. Sorting GPI-anchored proteins. *Nat Rev Mol Cell Biol* 2004;5:110–120.
2. Robinson MS. Adaptable adaptors for coated vesicles. *Trends Cell Biol* 2004;14:167–174.
3. Hicke L, Dunn R. Regulation of membrane protein transport by ubiquitin and ubiquitin-binding proteins. *Annu Rev Cell Dev Biol* 2003;19:141–172.
4. Bonifacino JS, Weissman AM. Ubiquitin and the control of protein fate in the secretory and endocytic pathways. *Annu Rev Cell Dev Biol* 1998;14:19–57.
5. Kerscher O, Felberbaum R, Hochstrasser M. Modification of proteins by ubiquitin and ubiquitin-like proteins. *Annu Rev Cell Dev Biol* 2006;22:159–180.
6. de Melker AA, van der Horst G, Calafat J, Jansen H, Borst J. c-Cbl ubiquitinates the EGF receptor at the plasma membrane and remains receptor-associated throughout the endocytic route. *J Cell Sci* 2001;114:2167–2178.
7. Huang F, Goh LK, Sorkin A. EGF receptor ubiquitination is not necessary for its internalization. *Proc Natl Acad Sci U S A* 2007;104:16904–16909.
8. Hawryluk MJ, Keyel PA, Mishra SK, Watkins SC, Heuser JE, Traub LM. Epsin 1 is a polyubiquitin-selective clathrin-associated sorting protein. *Traffic* 2006;7:262–281.
9. Fisher RD, Wang B, Alam SL, Higginson DS, Robinson H, Sundquist WI, Hill CP. Structure and ubiquitin binding of the ubiquitin-interacting motif. *J Biol Chem* 2003;278:28976–28984.
10. Katz M, Shtiegman K, Tal-Or P, Yakir L, Mosesson Y, Harari D, Machluf Y, Asao H, Jovin T, Sugamura K, Yarden Y. Ligand-independent degradation of epidermal growth factor receptor involves receptor ubiquitylation and Hgs, an adaptor whose ubiquitin-interacting motif targets ubiquitylation by Nedd4. *Traffic* 2002;3:740–751.
11. Klapisz E, Sorokina I, Lemeer S, Pijnenburg M, Verkleij AJ, van Bergen en Henegouwen PM. A ubiquitin-interacting motif (UIM) is essential for Eps15 and Eps15R ubiquitination. *J Biol Chem* 2002;277:30746–30753.
12. Polo S, Sigismund S, Faretta M, Guidi M, Capua MR, Bossi G, Chen H, De Camilli P, Di Fiore PP. A single motif responsible for ubiquitin recognition and monoubiquitination in endocytic proteins. *Nature* 2002;416:451–455.
13. Miller SL, Malotky E, O'Bryan JP. Analysis of the role of ubiquitin-interacting motifs in ubiquitin binding and ubiquitylation. *J Biol Chem* 2004;279:33528–33537.
14. Oved S, Mosesson Y, Zwang Y, Santonico E, Shtiegman K, Marmor MD, Kochupurakkal BS, Katz M, Lavi S, Cesareni G, Yarden Y. Conjugation to Nedd8 instigates ubiquitylation and down-regulation of activated receptor tyrosine kinases. *J Biol Chem* 2006;281:21640–21651.
15. Hurley JH, Emr SD. The ESCRT complexes: structure and mechanism of a membrane-trafficking network. *Annu Rev Biophys Biomol Struct* 2006;35:277–298.
16. Williams RL, Urbe S. The emerging shape of the ESCRT machinery. *Nat Rev Mol Cell Biol* 2007;8:355–368.
17. Field MC, Gabernet-Castello C, Dacks JB. 'Reconstructing the evolution of the endocytic system: insights from genomics and molecular cell biology'. *Adv Exp Med Biol* 2007;607:84–96.
18. Dacks JB, Field MC. Evolution of the eukaryotic membrane-trafficking system: origin, tempo and mode. *J Cell Sci* 2007;120:2977–2985.
19. Ferguson MA. The structure, biosynthesis and functions of glycosyl-phosphatidylinositol anchors, and the contributions of trypanosome research. *J Cell Sci* 1999;112:2799–2809.
20. Field MC, Carrington M. Intracellular membrane transport systems in *Trypanosoma brucei*. *Traffic* 2004;5:905–913.

21. Tazeh NN, Bangs JD. Multiple motifs regulate trafficking of the LAMP-like protein p67 in the ancient eukaryote *Trypanosoma brucei*. *Traffic* 2007;8:1007–1017.
22. Allen CL, Goulding D, Field MC. Clathrin-mediated endocytosis is essential in *Trypanosoma brucei*. *EMBO J* 2003;22:4991–5002.
23. Allen CL, Liao D, Chung WL, Field MC. Dileucine signal-dependent and AP-1-independent targeting of a lysosomal glycoprotein in *Trypanosoma brucei*. *Mol Biochem Parasitol* 2007;156:175–190.
24. Morgan GW, Goulding D, Field MC. The single dynamin-like protein of *Trypanosoma brucei* regulates mitochondrial division and is not required for endocytosis. *J Biol Chem* 2004;279:10692–10701.
25. Denny PW, Field MC, Smith DF. GPI-anchored proteins and glycoconjugates segregate into lipid rafts in Kinetoplastida. *FEBS Lett* 2001;491:148–153.
26. Grunfelder CG, Engstler M, Weise F, Schwarz H, Stierhof YD, Morgan GW, Field MC, Overath P. Endocytosis of a glycosylphosphatidylinositol-anchored protein via clathrin-coated vesicles, sorting by default in endosomes, and exocytosis via RAB11-positive carriers. *Mol Biol Cell* 2003;14:2029–2040.
27. Ziegelbauer K, Overath P. Identification of invariant surface glycoproteins in the bloodstream stage of *Trypanosoma brucei*. *J Biol Chem* 1992;267:10791–10796.
28. Chung WL, Carrington M, Field MC. Cytoplasmic targeting signals in transmembrane invariant surface glycoproteins of trypanosomes. *J Biol Chem* 2004;279:54887–54895.
29. Hua S, To WY, Nguyen TT, Wong ML, Wang CC. Purification and characterization of proteasomes from *Trypanosoma brucei*. *Mol Biochem Parasitol* 1996;78:33–46.
30. Li Z, Wang CC. Functional characterization of the 11 non-ATPase subunit proteins in the trypanosome 19 S proteasomal regulatory complex. *J Biol Chem* 2002;277:42686–42693.
31. Hein C, Springael JY, Volland C, Haguenaer-Tsapis R, Andre B. NPI1, an essential yeast gene involved in induced degradation of Gap1 and Fur4 permeases, encodes the Rsp5 ubiquitin-protein ligase. *Mol Microbiol* 1995;18:77–87.
32. Galan JM, Moreau V, Andre B, Volland C, Haguenaer-Tsapis R. Ubiquitination mediated by the Npi1p/Rsp5p ubiquitin-protein ligase is required for endocytosis of the yeast uracil permease. *J Biol Chem* 1996;271:10946–10952.
33. Morvan J, Froissard M, Haguenaer-Tsapis R, Urban-Grimal D. The ubiquitin ligase Rsp5p is required for modification and sorting of membrane proteins into multivesicular bodies. *Traffic* 2004;5:383–392.
34. Wang G, McCaffery JM, Wendland B, Dupre S, Haguenaer-Tsapis R, Huijbregtse JM. Localization of the Rsp5p ubiquitin-protein ligase at multiple sites within the endocytic pathway. *Mol Cell Biol* 2001;21:3564–3575.
35. Haglund K, Sigismund S, Polo S, Szymkiewicz I, Di Fiore PP, Dikic I. Multiple monoubiquitination of RTKs is sufficient for their endocytosis and degradation. *Nat Cell Biol* 2003;5:461–466.
36. Rubin C, Gur G, Yarden Y. Negative regulation of receptor tyrosine kinases: unexpected links to c-Cbl and receptor ubiquitylation. *Cell Res* 2005;15:66–71.
37. Thien CB, Langdon WY. Cbl: many adaptations to regulate protein tyrosine kinases. *Nat Rev Mol Cell Biol* 2001;2:294–307.
38. Ingham RJ, Gish G, Pawson T. The Nedd4 family of E3 ubiquitin ligases: functional diversity within a common modular architecture. *Oncogene* 2004;23:1972–1984.
39. Leung KF, Dacks JB, Field MC. Evolution of the multivesicular body ESCRT machinery; retention across the eukaryotic lineage. *Traffic* 2008; doi: 10.1111/j.1600-0854.2008.00797.x
40. McGrath JP, Jentsch S, Varshavsky A. UBA 1: an essential yeast gene encoding ubiquitin-activating enzyme. *EMBO J* 1991;10:227–236.
41. Handley PM, Mueckler M, Siegel NR, Ciechanover A, Schwartz AL. Molecular cloning, sequence, and tissue distribution of the human ubiquitin-activating enzyme E1. *Proc Natl Acad Sci U S A* 1991;1:258–262.
42. Jin J, Li X, Gygi SP, Harper JW. Dual E1 activation systems for ubiquitin differentially regulate E2 enzyme charging. *Nature* 2007;447:1135–1138.
43. Pelzer C, Kassner I, Matentzoglou K, Singh RK, Wollscheid HP, Scheffner M, Schmidtke G, Groettrup M. UBE1L2, a novel E1 enzyme specific for ubiquitin. *J Biol Chem* 2007;282:23010–23014.
44. Nolan DP, Geuskens M, Pays E. N-linked glycans containing linear poly-N-acetylglucosamine as sorting signals in endocytosis in *Trypanosoma brucei*. *Curr Biol* 1999;9:1169–1172.
45. Pal A, Hall BS, Nesbeth DN, Field HI, Field MC. Differential endocytic functions of *Trypanosoma brucei* Rab5 isoforms reveal a glycosylphosphatidylinositol-specific endosomal pathway. *J Biol Chem* 2002;277:9529–9539.
46. Pal A, Hall BS, Jeffries TR, Field MC. Rab5 and Rab11 mediate transferrin and anti-variant surface glycoprotein antibody recycling in *Trypanosoma brucei*. *Biochem J* 2003;374:443–451.
47. Ackers JP, Dhir V, Field MC. A bioinformatic analysis of the RAB genes of *Trypanosoma brucei*. *Mol Biochem Parasitol* 2005;141:89–97.
48. Seyfang A, Mecke D, Duzsenko M. Degradation, recycling, and shedding of *Trypanosoma brucei* variant surface glycoprotein. *J Protozool* 1990;37:546–552.
49. Terrell J, Shih S, Dunn R, Hicke L. A function for monoubiquitination in the internalization of a G protein-coupled receptor. *Mol Cell* 1998;1:193–202.
50. Barriere H, Nemes C, Lechardeur D, Khan-Mohammad M, Fruh K, Lukacs GL. Molecular basis of oligoubiquitin-dependent internalization of membrane proteins in mammalian cells. *Traffic* 2006;7:282–297.
51. Urbe S, Sachse M, Row PE, Preisinger C, Barr FA, Strous G, Klumperman J, Clague MJ. The UIM domain of Hrs couples receptor sorting to vesicle formation. *J Cell Sci* 2003;116:4169–4179.
52. Hirumi H, Hirumi K. Axenic culture of African trypanosome bloodstream forms. *Parasitol Today* 1994;10:80–84.
53. Wirtz E, Leal S, Ochatt C, Cross GA. A tightly regulated inducible expression system for conditional gene knock-outs and dominant-negative genetics in *Trypanosoma brucei*. *Mol Biochem Parasitol* 1999;99:89–101.
54. Redmond S, Vadivelu J, Field MC. RNAit: an automated web-based tool for the selection of RNAi targets in *Trypanosoma brucei*. *Mol Biochem Parasitol* 2003;128:115–118.
55. Nolan DP, Jackson DG, Biggs MJ, Brabazon ED, Pays A, Van Laethem F, Paturiaux-Hanocq F, Elliott JF, Voorheis HP, Pays E. Characterization of a novel alanine-rich protein located in surface microdomains in *Trypanosoma brucei*. *J Biol Chem* 2000;275:4072–4080.
56. Subramaniam C, Veazey P, Redmond S, Hayes-Sinclair J, Chambers E, Carrington M, Gull K, Matthews K, Horn D, Field MC. Chromosome-wide analysis of gene function by RNA interference in the African trypanosome. *Eukaryot Cell* 2006;5:1539–1549.